A novel onco-miR-365 induces cutaneous squamous cell carcinoma

Meijuan Zhou[1,†], Weilin Liu[1,†], Shudong Ma[2,†], Hong Cao[3],
Xuebiao Peng[4], Ling Guo[1,5], Xinhua Zhou[6], Li Zheng[1],
Linlang Guo[7], Miaojian Wan[8], Weimin Shi[9], Yingjie He[1,10],
Chao Lu[1], Lihong Jiang[1], Chengshan Ou[1], Yuanxia Guo[1]
and Zhenhua Ding[1,*]

[1]Department of Radiation Medicine, School of Public Health and Tropic
Medicine, Southern Medical University, Guangdong, Guangzhou 510515,
People's Republic of China, [2]Department of Oncology, Nanfang Hospital,
Guangdong, Guangzhou 510515, People's Republic of China, [3]Department
of Microbiology, School of Public Health and Tropic Medicine, Southern
Medical University, Guangdong, Guangzhou 510515, People's Republic
of China, [4]Department of Dermatology, Nanfang Hospital, Guangdong,
Guangzhou 510515, People's Republic of China, [5]Division of Life and Health
Sciences, Tsinghua Campus, The University Town, Guangdong, Shenzhen
518055, People's Republic of China, [6]Department of Pathology, Nanfang
Hospital, Guangdong, Guangzhou 510515, People's Republic of China,
[7]Department of Pathology, Zhujiang Hospital, Guangadong, Guangzhou
510280, People's Republic of China, [8]Department of Dermatology, The
Third Hospital Affiliated to Sun Yat-sen University, Guangdong, Guangzhou
510630, People's Republic of China, [9]Department of Oncology, Guangdong
No. 2 Provincial People's Hospital, Guangdong, Guangzhou 510317,
People's Republic of China and [10]Department of Radiation Protection,
Chongqing CDC, Chongqing 400042, People's Republic of China

*To whom correspondence should be addressed. Tel: +86-20-61648315;
Fax: +86-20-61648324;
Email: dingzh@smu.edu.cn

The expression levels of miR-365 vary in different malignancies.
Herein, we found that miR-365 was overexpressed in both cells
and clinical specimens of cutaneous squamous cell carcinoma
(SCC). We demonstrated that the HaCaT$^{pre-miR-365-2}$ cell line, which
overexpressed miR-365, could induce subcutaneous tumors *in
vivo*. Antagomir-365, an anti-miR-365 oligonucleotide, inhibited
cutaneous tumor formation *in vivo*, along with G_1 phase arrest
and apoptosis of cancer cells. These findings suggest that miR-
365 may act as an onco-miR in cutaneous SCC both *in vitro* and
in vivo. The present study provides valuable insight into the role
of miR-365 in cutaneous SCC formation, which can help develop
new drug and miR-365 target-based therapies for cutaneous SCC.

Introduction

Mutation or abnormal expression of micro-RNAs (miRNAs), which
can function as either tumor suppressors or oncogenes, is implicated
in various cancers (1–4). miRNAs act as an oncogene in tumors
mainly via repressing tumor suppressors or inducing mutations of
tumor suppressor genes (5). miRNAs are a family of ~22 non-protein-
coding small RNA molecules that act as a class of RNA-interference
agents (6). They negatively regulate the levels of their target proteins,
mainly by annealing with 3′ untranslated region of the target genes
(7,8), to regulate the cellular proliferation, differentiation and apopto-
sis (9,10). About 40% of the confirmed miRNAs in the genome have
been found to be related to the occurrence or/and development of can-
cer. For example, miR-21 and miR-155 are overexpressed in breast
cancer and diffuse large B-cell lymphoma, respectively (11–13). Let-
7, on the other hand, can inhibit the proliferation of lung cancer cells
by downregulating RAS expression and act as a tumor suppressor
gene (14,15). Thus, there is great interest in determining the role of

miRNAs in the pathology, classification, diagnosis and treatment of
cancers (11,16,17).

miR-365 is located in the chromosome region 16p13.12, and the
sequence of matured hsa-miR-365 is sheared from two precursors:
hsa-mir-365-1 and hsa-mir-365-2. It has been reported that miR-365 is
overexpressed in human breast cancer and downregulates interleukin-6
levels in cooperation with Sp1 and nuclear factor kappaB in HeLa cells
(18,19). Moreover, miR-365 has been reported to be involved in signal
transduction in the carcinogenesis of small cell lung cancer and colo-
rectal cancer (20). In a prior study in which we analyzed the miRNA
expression profile of the NIH 3T3 cell line after irradiation with ultravi-
olet B, we found that miR-365 was one of the most sensitive miRNAs to
ultraviolet B irradiation. We, therefore, hypothesize that miR-365 may
play an important role in the development of skin cancer.

In the present study, we investigated the function of miR-365 in
cutaneous squamous cell carcinoma (SCC), the second most common
skin cancer.

Materials and methods

This study was approved by the Institutional Review Board of our hospital, and
all patients provided written informed consent for the use of surgical samples.
All animals were treated according to standard guidelines for the use and care
of laboratory animals.

Cell culture and tumor samples

Cutaneous SCC lines A431, Tca8113, SCC13, HSC-5 (China Center for
Type Culture Collection and Cell Bank of the Chinese Academy of Sciences,
Shanghai, China) and HSC-1 (Dongguang Biojet Biotech. Co., Ltd,
Guangzhou, China) and human benign epidermal keratinocyte cell line HaCaT
(China Center for Type Culture Collection, Wuhan, China) were cultured in
Dulbecco's modified Eagle medium (DMEM) supplemented with 10% fetal
bovine serum, 100 units/ml penicillin and streptomycin (Invitrogen, Carlsbad,
CA) and maintained at 37°C with 5% CO_2 in a humidified atmosphere.

Cutaneous SCC samples were obtained from patients diagnosed with cuta-
neous SCC from January 2009 to August 2011 in the departments of derma-
tology, pathology and oncology at Nanfang Hospital and Zhujiang Hospital,
affiliated to Southern Medical University and The Third Affiliated Hospital
to Sun Yat-sen University. A total of 108 specimens of cutaneous SCC were
included in the analysis (69 samples from males and 39 from females). Biopsy
specimens were collected from patients (fresh biopsies, $n = 37$), and formalin-
fixed paraffin-embedded specimens were collected from the archive ($n = 71$).
Approximately 74% of the patients were >50 years of age. Adjacent non-
cancerous tissue samples were used as normal control tissues. Fresh samples
taken from the surgery were immediately frozen in liquid nitrogen for subse-
quent total RNA extraction and paraffin embedding. Tumors were classified
according to the SCC Broders Pathological Classification: stage I (well differ-
entiated) with 0–5% undifferentiated cells, stages II–III (moderately differenti-
ated) with 25–75% undifferentiated cells and stage IV (poorly differentiated)
with 75–100% undifferentiated cells. Of the 108 cases, 78 cases were well
differentiated (72.22%), 26 moderately differentiated (24.07%) and 4 poorly
differentiated (3.07%). The proliferative marker Ki-67 was used to confirm the
differentiation status of the tumors and on average the expression was 80–90%
positive. Tumor data are summarized in Table I.

Isolation of RNA and quantitative real-time-PCR

Total RNAs of the cutaneous SCC cell lines (2×10^6 cells) and tissues (100 mg)
were extracted with Trizol (Invitrogen) according to the manufacturer's proto-
col. The RNA was quantified by absorption at 260 nm. The reverse-transcrip-
tion reaction and quantitative real-time PCR (qRT-PCR) were performed with
a TaqMan qRT-PCR kit (Takara Bio, Shiga, JP) and TaqMan microRNA assay
(Ambion, Austin, TX).

Primer sequences for pre-miR-365 were designed using Primer
Express Software from Applied Biosystems. The following forward and
reverse primers were used for amplification—pre-miR-365-1, forward:
5′-AGGTCCCTTTCGTGAGTC-3′ and reverse: 5′-GCTACAGCGGA
AGAGTTT-3′; pre-miR-365-2, forward: 5′-TCACCTCGGCTCATCTGG-3′
and reverse: 5′-TGACCTTCCTTGGGCACT-3′; GAPDH, forward:
5′-GAAGGTGAAGGTCGG AGTC-3′ and reverse: 5′-GAAGATGGTGAT
GGGATTTC-3′ and mature miR-365 primer (Ambion). Reactions were

Abbreviations: DMEM, Dulbecco's modified Eagle medium; miRNA,
micro-RNA; qRT-PCR, quantitative real-time PCR; SCC, squamous cell
carcinoma

†These authors contributed equally to this work.

Table I. Clinicopathological data of SCC (*n* = 108)

Clinical outcome	Number	Ki-67 staining	miRNA-365 FISH
Gender			
Male	69 (63.89%)	++ (80–90%)	++ (70–80%)
Female	39 (26.11%)	++ (80–90%)	++ (70–80%)
Age (years)			
>50	80 (74.07%)	++ (80–90%)	++ (70–80%)
≤50	28 (25.93%)	++ (80–90%)	++ (70–80%)
Tumor size (cm)			
>3	24 (23.22%)	++ (80–90%)	++ (70–80%)
≤3	84 (77.78%)	++ (80–90%)	++ (70–80%)
Histologic cell type			
Well differentiated	78 (72.22%)	++ (80–90%)	++ (80–90%)
Moderately differentiated	26 (24.07%)	++ (70–80%)	++ (60–70%)
Poorly differentiated	4 (3.71%)	++ (50–60%)	++ (30–40%)
Lymph node metastasis			
Absent	101 (93.52%)	++ (80–90%)	++ (70–80%)
Present	7 (6.48%)	++ (80–90%)	−− (0–10%)
Venous invasion			
Absent	3 (2.78%)	++ (20–30%)	−− (0–10%)
Present	105 (97.22%)	++ (80–90%)	++ (70–80%)

performed on a Stratagene MX3005P instrument. Cycling parameters were 95°C for 10 min, 40 cycles of 95°C (15 s) and annealed/extended at 60°C for 1 min. The gene expression △△Ct values of miRNAs from each sample were calculated by normalizing with internal control U6 rRNA (Ambion). The △△Ct was calculated by subtracting the Ct of U6 rRNA from the Ct of the miRNA of interest. Fold change was calculated using the equation $2^{-\triangle\triangle Ct}$. All experiments were performed in triplicate.

miRNA-FISH

The formalin-fixed paraffin-embedded cutaneous SCC was used for miRNA hybridization. Specimen was deparaffinized and hydrated, followed by treatment with proteinase K and refixation in 4% paraformaldehyde. After washing with phosphate-buffered saline and air-drying, the sections were hybridized with 10 nM DIG-labeled LNA-miR-365 probe that was prepared by a DIG-3′ and 5′-end labeling kit (Exiqon, Vedbaek, Denmark) following the manufacturer's protocol (www.exiqon.com) before they were stained with the fluorescein isothiocyanate-labeled LNA-miR-365 probe. Nuclei were routinely stained using 4′,6-diamidino-2-phenylindole.

HaCaT$^{pre-miR-365-2}$ cell line construction

The pre-miR-365-2 cDNA was obtained from NCBI (NC_000017.10), and three cDNA fragments were amplified by PCR. A 971 bp fragment was first amplified with the forward pre-miR-365-2 (5′-CGCGGATCCTGGCTGTCTTGTGTTCATGT-3′) and the reverse pre-miR-365-2 (5′-CCGGAATTCTCCTCTACTCCTGCCTCAAC-3′) primers. The obtained DNA was then digested with BamHI and EcoRI and cloned in pBabe-puro vector. Next, the pBabe-puro-miR-365-2 plasmid was obtained by T4 DNA (TaKaRa) conjunction and DH5α transformation before all constructs were confirmed by DNA sequencing. Then retrovirus package pBabe-puro-miR-365-2 or empty vector in 293FT cell line was obtained by calcium phosphate precipitate. The HaCaT cell line was infected by the supernatant containing virus before the cells were screened by puromycin. The pre-miR-365-2 and miR-365 expressions in HaCaT$^{pre-miR-365-2}$ and HaCaT$^{pBabe-puro}$ cell lines were confirmed by qRT-PCR.

Western blotting

Western blot analysis was performed as described by Ding *et al.* (21), with minor modifications. Briefly, total cellular proteins (20 µg) were electrophoresed through a 10% denaturing polyacrylamide gel and transferred to a nitrocellulose membrane (Schleicher & Schuell, Keene, NH). The blots were probed with the anti-NFIB or anti-β-actin (Abcam, Cambridge, MA) and the bound antibody was detected using an ECL Plus kit (GE Healthcare, Buckinghamshire, UK) according to the manufacturer's protocol.

Tumorigenicity assay in nude mice

Six-week-old BALB/c-nu mice were subcutaneously injected with 2×10^7 cells of the lines HaCaT$^{pre-miR-365-2}$ (*n* = 13) and HaCaT$^{pBabe-puro}$ (*n* = 4), respectively, in the right back flank. Tumor size was assessed every other day by caliper measurement. Tumor volume was calculated as follows: volume = $D \times d^2 \times \pi/6$, where *D* and *d* are the longer and the shorter diameters, respectively. Tumors were taken from representative BALB/c-nu mice 21 days after injection with HaCaT$^{pre-miR-365-2}$ cells. For survival analysis, mice were killed when tumors reached a volume of 500 mm³.

Treatment of antagomir-365 in vitro and in vivo

Antagomirs were synthesized by RiboBio Co. (Guangzhou, China), and the sequences were 5′-APSUPSUPSAPSCGGGGAUUUUUAGGAAUPSAPS–Chol-3′ (antagomir-365). The A431 cell line was seeded in antibiotic-free media in 6-well plates (2×10^6 cells/well) and treated for 24 h with antagomir-365 at a final concentration of 100 nM, or with an equal volume of phosphate-buffered saline, when the cells were at 50–60% of confluence.

The A431 cell line (2×10^7 cells) was subcutaneously injected into the right back flank of 5-week-old BALB/c-nu mice. After 1 week, when the tumors reached an average volume of 150 mm³, antagomir-365 (25 nM of antagomir-365 diluted in 100 µl phosphate-buffered saline; *n* = 7), control without antagomir (*n* = 3), was injected intratumorally three times per week for 2 weeks. Tumor diameters were measured every 2 days.

Cell cycle analysis and apoptosis detection

Cell cycles were analyzed by flow cytometry. The cells were fixed in chilled 70% ethanol for at least 24 h before staining with 100 µg/ml propidium iodide and 100 µg/ml RNase A (Sigma, St Louis, MO) and were analyzed using FACScan (Beckman Coulter, Fullerton, CA) after staining for 30 min. All experiments were performed in triplicate.

Apoptosis was detected with the TUNEL apoptosis detection kit (Promega) according to manufacturer's protocol. Briefly, cells were stained with TdT (fluorescent labeling) and 4′,6-diamidino-2-phenylindole and analyzed using a fluorescence microscope (Olympus, Japan).

Migration and Matrigel invasion assays

In vitro analysis of tumor cell migration was carried out using transwell migration. In the transwell migration assay, cells (1×10^6/ml) in 100 µl DMEM were seeded to the upper chamber (Costar, Lowell, MA) and 500 µl DMEM (containing 10% fetal bovine serum) was added into the lower chamber (containing a porous membrane with 8 µm diameter pores) and incubated at 37°C with 5% CO_2 in a humidified atmosphere. Migration was measured 24 h later.

The Matrigel invasion assay was performed using the cell invasion assay kit (Chemicon, Temecula, CA) according to manufacture's protocol. Cells (1×10^6) in 300 µl DMEM were seeded in the upper chamber and 500 µl DMEM (containing 10% fetal bovine serum) was added into the lower chamber. The Matrigel invasion chamber was then incubated for 24 h in a tissue culture incubator, and then the non-invading cells as well as the ECMatrix gel were gently removed from the interior of the insert using a cotton-tipped swab. Invasive cells on the lower surface of the membrane were stained by placing the inserts in the staining solution for 20 min. The inserts were then dipped in a beaker of water three times to rinse and allowed to air dry. The invasion rate was determined by counting the stained cells.

Statistical analysis

Data were presented as mean ± standard deviation. The groups were compared by one-way analysis of variance using SNK-*q* test or by the *t*-test with two-tailed *P* value. Survival data were presented as Kaplan–Meier plots and were analyzed using a log-rank (Mantel–Haenszel) method. The significance level was *P* < 0.05.

Results

miR-365 is overexpressed in cutaneous SCC

To understand the role of miR-365 in the development of cutaneous SCC, the expressions of miR-365 in 37 cutaneous SCC and 1 human benign epidermal keratinocyte cell line, HaCaT, and 5 cutaneous SCC cell lines, A431, HSC-1, Tca8113, SCC13 and HSC-5, were first examined by qRT-PCR. As shown in Figure 1A, miR-365 expression was elevated compared with the adjacent control in 72% of the clinical SCC cases. For miR-365 expression in cell lines, the results showed that compared with the control cell line HaCaT, the expressions of miR-365 were markedly increased in all five SCC cell lines, with a maximum increase of over 15-fold in A431 (15.67 ± 1.12, *P* < 0.001) and a minimum increase of almost 5-fold in Tca8113 (4.72 ± 0.85, *P* < 0.05) (Figure 1B).

Next, using miRNA-FISH, we detected the expression of miR-365 in cutaneous SCC (37 fresh, 71 paraffin embedded). miR-365 positive expression was detected in 72.5% of the 37 fresh SCC samples (representative photos are shown in Figure 1C). The association between miR-365 expression and differentiation status of the cutaneous SCC was determined, and the results showed that the positive index of miR-365 was remarkably higher (76.8% on average) in tumors that exhibited venous invasion than in those without venous
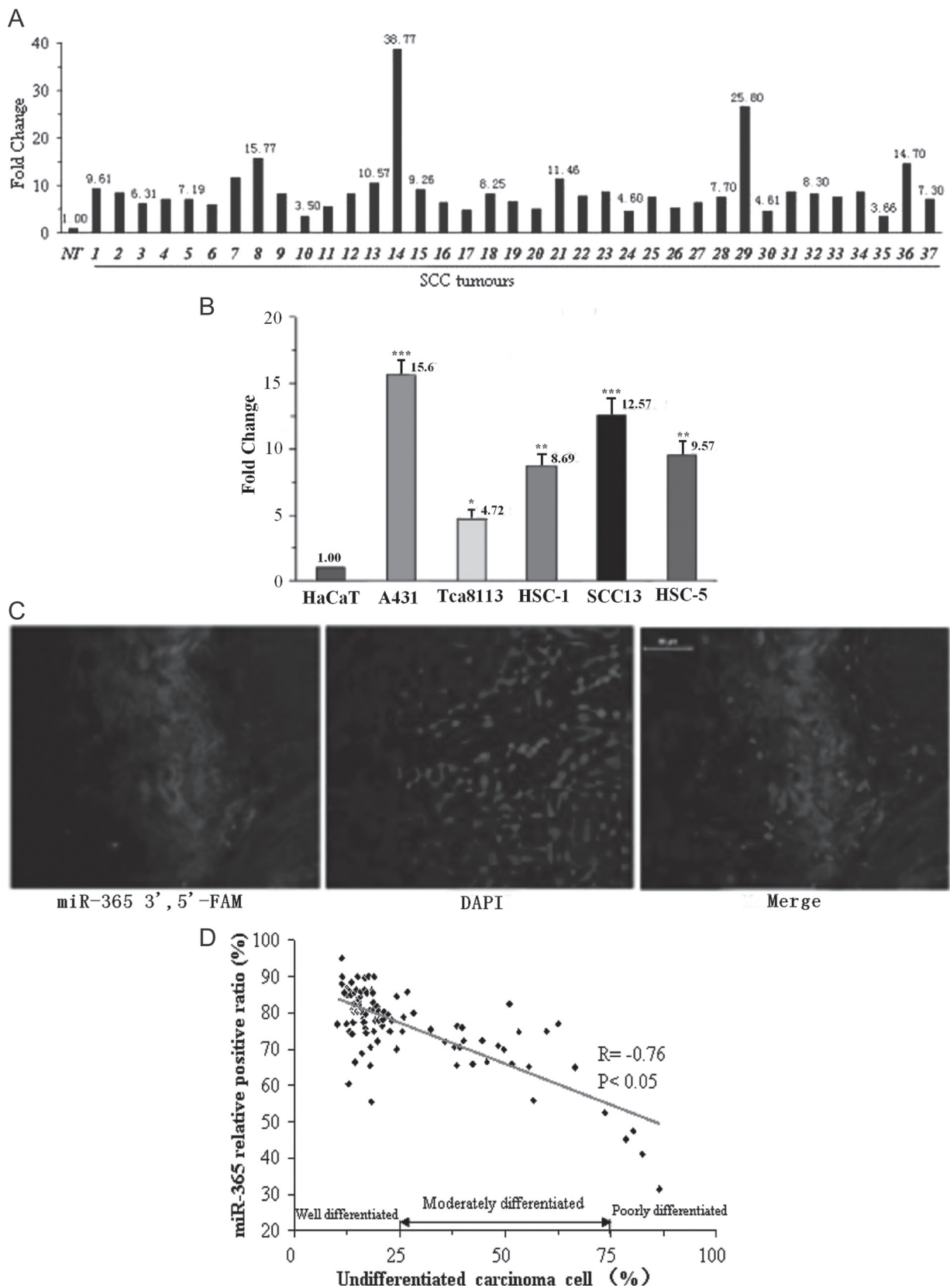
Fig. 1. miR-365 is overexpressed in cutaneous SCC. (**A**) miR-365 expression in fresh cutaneous SCC compared with adjacent non-cancerous tissue samples by qRT-PCR (*n* = 37; *y*-axis denotes fold change). (**B**) qRT-PCR analysis of miR-365 expression in different cutaneous SCC cell lines: A431, HSC-1, SCL-1, SCC13 and HSC-5, and human benign epidermal keratinocyte cell line HaCaT (*y*-axis denotes fold change). Means ± SD are shown for all panels. *$P < 0.05$; **$P < 0.01$; ***$P < 0.001$ (*n* = 3). (**C**) A representative sample of hsa-miR-365 expression by *in situ* hybridization with mercury LNA™ micro-RNA. (**D**) The correlation of miR-365 positive expression with the cutaneous SCC histological differentiation (*n* = 108).
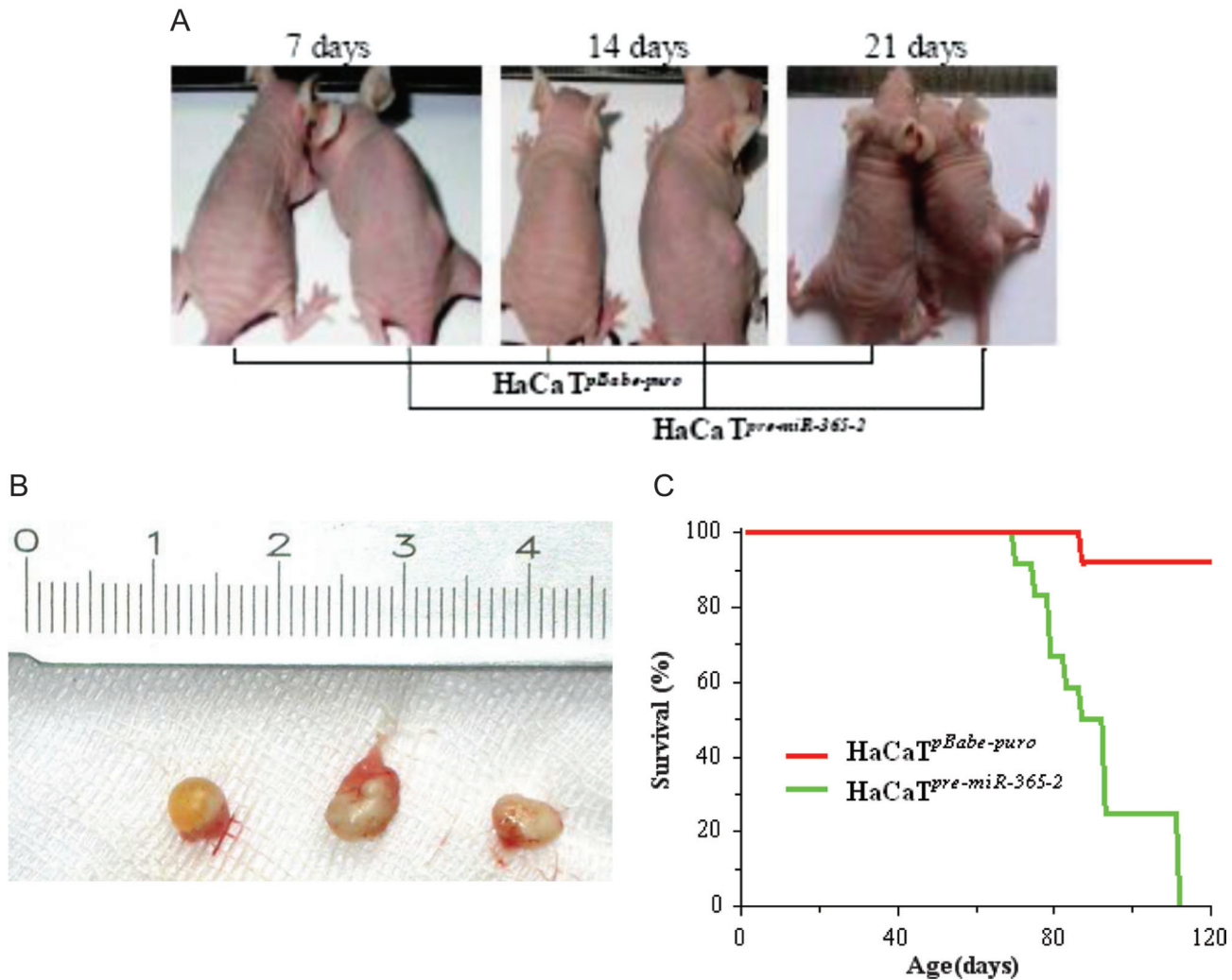
Fig. 2. HaCaT[pre-miR-365-2] cells overexpressed miR-365 and induced tumors in nude mice. (**A**) Time course of tumor induction of a representative BALB/c-nu mouse. Nude mice were injected with HaCaT[pBabe-puro] cells (pBabe-puro empty vector in HaCaT cells, left mouse; $n = 4$) or HaCaT[pre-miR-365-2] cells (right mouse; $n = 13$). (**B**) Tumors at the right flank from representative BALB/c-nu mice 21 days after injection with HaCaT[pre-miR-365-2] cells (all tumors are from 21 days after injection). (**C**) Percentages of survival for 4 months ($n = 13$).

invasion in which miR-365 was hardly expressed (Table I). Moreover, no overexpression of miR-365 was detected in the metastatic lymph nodes of SCC (seven cases in all; Table I). There was an inverse correlation between the miR-365 expression level and differentiation of cutaneous SCC cells ($R = -0.76$, $P < 0.05$) (Figure 1D).

Tumorigenicity of miR-365 in nude mice
Stable cell lines with empty vector control (HaCaT[pBabe-puro]) and pre-miR-365 overexpression (HaCaT[pre-miR-365-2]) were constructed. As shown in Supplementary Figure 1A, available at *Carcinogenesis* Online, the expression of pre-miR-365-2 and miR-365 in the HaCaT[pre-miR-365-2] cell line was increased by 64 and 37 times, respectively (64.18 ± 0.97, $P < 0.001$; 37.47 ± 1.01, $P < 0.001$). In addition, the HaCaT[pre-miR-365-2] cell line featured increases in proliferation, migration and invasion *in vitro*, which are the characteristics of malignant phenotype of cancer cells, compared with the HaCaT[pBabe-puro] cell line (Supplementary Figure 1B–D, available at *Carcinogenesis* Online).

HaCaT[pre-miR-365-2] was then used to induce subcutaneous tumors in 13 BALB/c-nu mice. Mice died 70–110 days after the tumor formation in their right back flank (Figure 2A). Resected tumors at 21 days of tumor formation are shown in Figure 2B. Approximately 50% of mice that received HaCaT[pre-miR-365-2] survived to 90 days, whereas 100% of those that received HaCaT[pBabe-puro] survived to 90 days (Figure 2C).

Antagomir-365 inhibits tumorigenesis in vitro and abolishes tumor growth in vivo
To determine whether miR-365 played a role in the occurrence of cutaneous SCC, we further applied anti-miR-365 oligonucleotides (antagomir-365) to suppress the growth of cutaneous SCC both *in vitro* and *in vivo*. After transfection of anti-miR-365 oligonucleotides (antagomir-365) in A431 cells, G_1 phase cell arrest and an increased apoptotic rate were noted (Figure 3A). Cell proliferation was suppressed compared with the control with no antagomir-365 (Figure 3B). Decrease in cell migration and invasion was noted after transfecting anti-miR-365 oligonucleotides (antagomir-365) in A431 cells (Figure 3C and D).

To further examine antagomir-365 function *in vivo*, subcutaneous SCC tumors formed by injection of 2×10^7 A431 cells into nude mice were challenged with silencing of miR-365 using antagomir-365 treatment. After the tumor volume reached >150 mm³ (22) at 8 days after injection, intratumoral multidot injection of antagomir-365 was performed. The tumor volume and apoptosis of the SCC cells were analyzed 2 weeks later. The results showed that tumor growth was significantly suppressed compared with the control group that did not receive injection of antagomir-365 (496.61 ± 42.5 versus 20.5 ± 14.89, $P < 0.001$) and was even abolished in one sample (Figure 3E). Apoptosis occurred in all A431 tumors treated with antagomir-365, with an
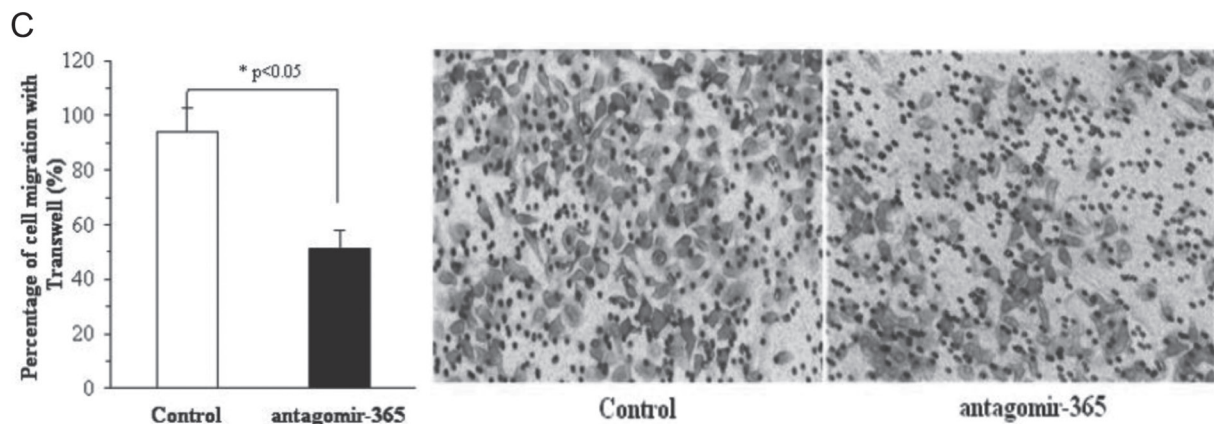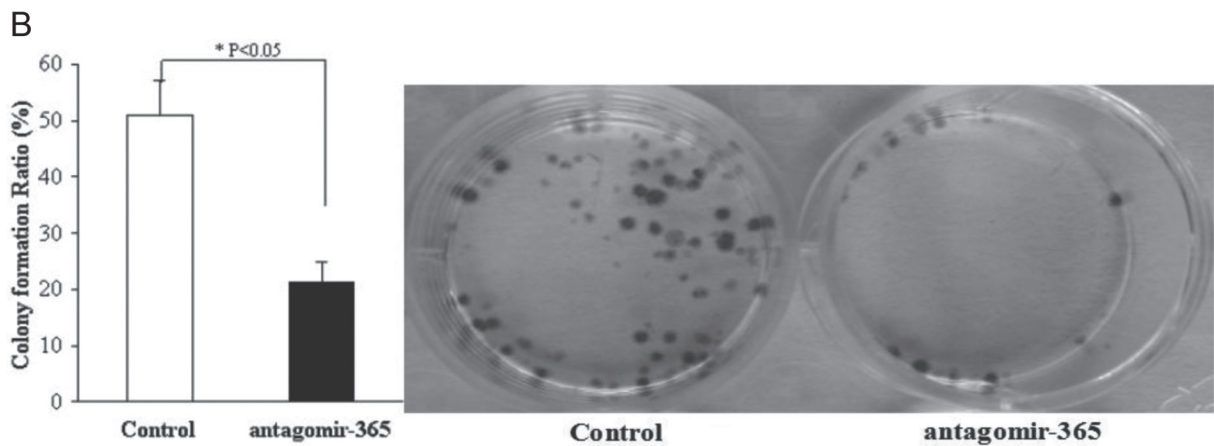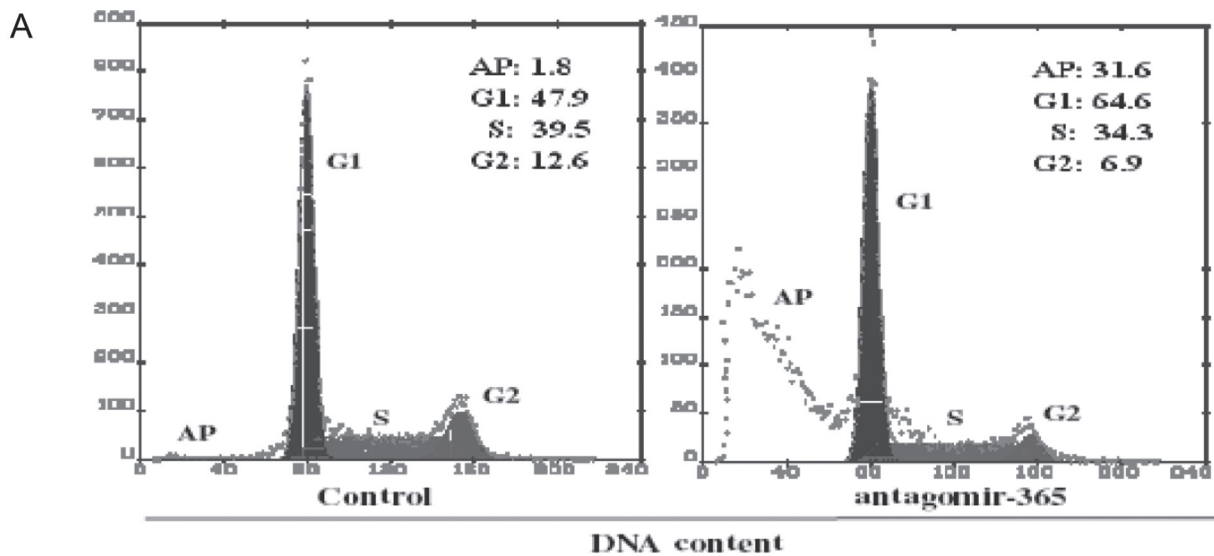
average apoptosis ratio of 85.6%, which was about 4-fold that of the control (0.856 ± 0.087 versus 0.167 ± 0.047, $P < 0.01$) (Figure 3F).

Discussion

miR-365 has been reported to be involved in the carcinogenesis of small cell lung cancer and colorectal cancer (23). The present study, to the best of our knowledge, is the first to report overexpression of miR-365 in both fresh and paraffin-embedded samples of cutaneous SCC. In order to further identify its role in the differentiation of cutaneous SCC cells, as well as in the genesis and progression of tumors, we constructed a cell line HaCaT$^{pre-miR-365-2}$ by overexpression

of pre-miR-365-2, resulting in malignant cancer cell formation and induction of subcutaneous tumors in nude mice. Further research is needed to explore the underlying functional mechanisms of the cell line. These findings strongly suggest that miR-365 is an oncogene in cutaneous SCC.

miR-365 has rarely been studied in cutaneous cancers, though it was reported as an apoptosis-promoting agent and a growth inhibitor in malignant melanoma (24,25). Our results, however, showed that miR-365 could act as an onco-miRNA. The discrepancy between our results and those of other studies may be due to the pre-miR-365-1 used in other reports (26) or the different types of skin cancers studied. In this study, we used pre-miR-365-2 to successfully construct a
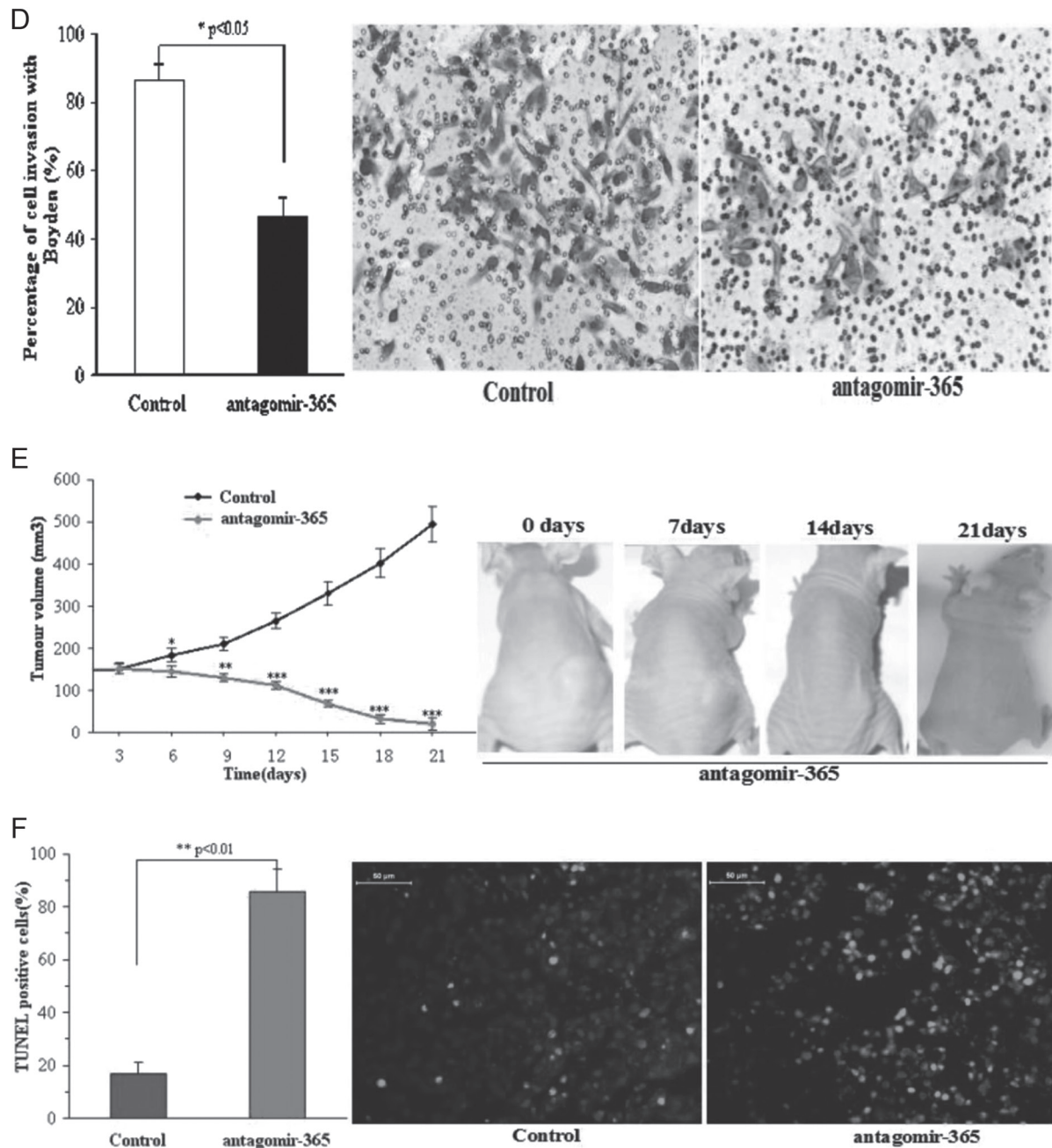
Fig. 3. Antagomir-365 inhibits tumorigenesis of A431 cells *in vitro* and abolishes A431 tumor growth *in vivo*. (**A**) The distribution of A431 cell cycles following treatment in the presence or absence of antagomir-365 by flow cytometry ($n = 3$). (**B**) Colony formation of the A431 cell line following mock transfection or transfection with antagomir-365 and then cultured for 14 days ($n = 4$). (**C**) Transwell migration assay of A431 cell line following mock transfection or transfection with antagomir-365 ($n = 4$). (**D**) Matrigel invasion assay of A431 cell line transfected with antagomir-365 and incubated for 24 h ($n = 4$). Control was mock transfected. (**E**) Changes of tumor volume in the absence or presence of antagomir-365 treatment with intratumoral multidot injection. The time course of tumor treatment with antagomir-365 is shown (red, $n = 7$) in comparison with the untreated control (black, $n = 3$) (top right). Tumors from representative mice 21 days after treatment are shown in the right-side panels. (**F**) Terminal deoxynucleotidyl transferase-mediated dUTP nick end labeling assay for apoptosis measurement of tumors with and without antagomir-365 treatment. $*P < 0.05$; $**P < 0.01$; Means ± standard deviation (SD) are shown for all panels.

new HaCaT$^{pre-miR-365-2}$ cell line, which expressed pre-miR-365-2 and the results indicated that miR-365 regulates NFIB protein expression (Supplementary Figure 2, available at *Carcinogenesis* Online).

NFIB is a member of the NFI gene family, which is composed of NFI-A, -B, -C, and -X in vertebrates and functions as a versatile transcriptional repressor of many promoters either through competition with other transcriptional factors for binding or through changes in the nucleosome structure (27). NFIB functions to enhance expressions of more than 100 genes in organs like the brain, lung, liver and intestine, and it regulates cell proliferation and differentiation in lung maturation (28,29). It has been reported that NFIB can react with miR-21 through a double-negative feedback loop (30) and is also a target gene of miRNAs-372/373 (31). The contradictions between our study and previous studies indicate the role of miR-365 in carcinogenesis may vary with its different precursors. Although so far there has been no research addressing the different roles of different precursors, we tentatively presume that the two different precursors of mature miR-365 may result in the different functions.

As miRNAs can function as key molecules in oncogenes and suppressors, they have been targeted in target-based therapies for various cancers (32). For example, antagomir-17-5p abolishes the growth of therapy-resistant neuroblastomas (22). miR-335-specific inhibitor antagomir-335 strongly blocks the malignant glioma cells (33). Similarly, the antagomir-365 can be used to suppress the growth of cutaneous SCC. Coincidentally, we found that antagomir-365 can upregulate the NFIB expression (Supplementary Figure 2, available at *Carcinogenesis* Online).

The present study has certain limitations. First, to better characterize miR-365, more downstream target genes of miR-365 should be investigated, including the NFIB gene. Second, future studies should include an examination of miR-365 expression in clinical blood samples to better determine any association between miR-365 and metastasis of cutaneous SCC.

Conclusions

In this study, we demonstrated that miR-365 was overexpressed both in fresh SCC samples and paraffin-embedded tissues and that miR-365 may act as an onco-miR in cutaneous SCC both *in vitro* and *in vivo*. Overexpression of miR-365 induced tumorigenicity of HaCaT cells, and silencing of miR-365 using an antagomir-365 could reduce A431 tumor growth *in vivo*. These findings demonstrate that miR-365 may be a carcinogenic factor in cutaneous SCC and a potential target in cutaneous SCC therapy. The overexpression of miR-365 in cutaneous SCC and its role in differentiation of cutaneous SCC cells as well as in the venous invasion of the tumor suggest that the expression level of miR-365 can be used as a potential indicator both in the clinical diagnosis and treatment.

Supplementary material

Supplementary Figures 1 and 2 can be found at http://carcin.oxford-journals.org/

References

1. Esquela-Kerscher,A. *et al.* (2006) Oncomirs—microRNAs with a role in cancer. *Nat. Rev. Cancer*, **6**, 259–269.
2. Kent,O.A. *et al.* (2006) Small piece in the cancer puzzle: microRNAs as tumor suppressors and oncogenes. *Oncogene*, **25**, 6188–6196.
3. Zhang,B. *et al.* (2006) MicroRNAs as oncogenes and tumor suppressors. *Dev. Biol.*, **302**, 1–12.
4. Calin,G.A. *et al.* (2004) MicroRNA genes are frequently located at fragile sites and genomic regions involved in cancers. *Proc. Natl Acad. Sci. U.S.A.*, **101**, 2999–3004.
5. Jiang,S. *et al.* (2010) MicroRNA-155 functions as an oncomiR in breast cancer by targeting the suppressor of cytokine signaling 1 gene. *Cancer Res.*, **70**, 3119–3127.
6. Siomi,M.C. *et al.* (2011) PIWI-interacting small RNAs: the vanguard of genome defence. *Nat. Rev. Mol. Cell Biol.*, **12**, 246–258.
7. He,L. *et al.* (2004) MicroRNAs: small RNAs with a big role in gene regulation. *Nat. Rev. Genet.*, **5**, 522–531.
8. Zhao,Y. *et al.* (2007) A developmental view of microRNA function. *Trends Biochem. Sci.*, **32**, 189–197.
9. Felli,N. *et al.* (2005) MicroRNAs 221 and 222 inhibit normal erythropoiesis and erythroleukemic cell growth via kit receptor down-modulation. *Proc. Natl Acad. Sci. U.S.A.*, **102**, 18081–18086.
10. He,L. *et al.* (2007) MicroRNAs join the p53 network—another piece in the tumour-suppression puzzle. *Nat. Rev. Cancer*, **7**, 819–822.
11. Volinia,S. *et al.* (2006) A microRNA expression signature of human solid tumors defines cancer gene targets. *Proc. Natl Acad. Sci. U.S.A.*, **103**, 2257–2261.
12. Iorio,M.V. *et al.* (2005) MicroRNA gene expression deregulation in human breast cancer. *Cancer Res.*, **65**, 7065–7070.
13. Eis,P.S. *et al.* (2005) Accumulation of miR-155 and BIC RNA in human B cell lymphomas. *Proc. Natl Acad. Sci. U.S.A.*, **102**, 3627–3632.
14. John,B. *et al.* (2004) Human microRNA targets. *PLoS Biol.*, **2**, e363.
15. Takamizawa,J. *et al.* (2004) Reduced expression of the let-7 microRNAs in human lung cancers in association with shortened postoperative survival. *Cancer Res.*, **64**, 3753–3756.
16. Medina,P.P. *et al.* (2010) OncomiR addiction in an *in vivo* model of microRNA-21-induced pre-B-cell lymphoma. *Nature*, **467**, 86–90.
17. Krützfeldt,J. *et al.* (2005) Silencing of microRNAs *in vivo* with 'antago-mirs'. *Nature*, **438**, 685–689.
18. Yan,L. *et al.* (2008) MicroRNA miR-21 overexpression in human breast cancer is associated with advanced clinical stage, lymph node metastasis and patient poor prognosis. *RNA*, **14**, 2348–2360.
19. Xu,Z. *et al.* (2011) MiR-365, a novel negative regulator of interleukin-6 gene expression, is cooperatively regulated by Sp1 and NF-kappaB. *J. Biol. Chem.*, **286**, 21401–21412.
20. Guo,L. *et al.* (2009) Differential expression profiles of microRNAs in NIH3T3 cells in response to UVB irradiation. *Photochem. Photobiol.*, **85**, 765–773.
21. Ding,Z. *et al.* (2002) Induction of apoptosis by the anticancer drug XK469 in human ovarian cancer cell lines. *Oncogene*, **21**, 4530–4538.
22. Fontana,L. *et al.* (2008) Antagomir-17-5p abolishes the growth of therapy-resistant neuroblastoma through p21 and BIM. *PLoS ONE*, **3**, e2236.
23. Guo,H. *et al.* (2011) MicroRNAs-372/373 promote the expression of hepatitis B virus through the targeting of nuclear factor I/B. *Hepatology*, **54**, 808–819.
24. Nie,J. *et al.* (2012) MicroRNA-365, down-regulated in colon cancer, inhibits cell cycle progression and promotes apoptosis of colon cancer cells by probably targeting cyclin D1 and Bcl-2. *Carcinogenesis*, **33**, 220–225.
25. Qin,B. *et al.* (2011) MicroRNAs expression in ox-LDL treated HUVECs: miR-365 modulates apoptosis and Bcl-2 expression. *Biochem. Biophys. Res. Commun.*, **410**, 127–133.
26. Papetti,M. *et al.* (2011) Mybl2, downregulated during colon epithelial cell maturation, is suppressed by miR-365. *Am. J. Physiol. Gastrointest. Liver Physiol.*, **301**, G508–G518.
27. Gronostajski,R.M. (2000) Roles of the NFI/CTF gene family in transcription and development. *Gene*, **249**, 31–45.
28. Hsu,Y.C. *et al.* (2011) Mesenchymal nuclear factor I B regulates cell proliferation and epithelial differentiation during lung maturation. *Dev. Biol.*, **354**, 242–252.
29. Persson,M. *et al.* (2009) Recurrent fusion of MYB and NFIB transcription factor genes in carcinomas of the breast and head and neck. *Proc. Natl Acad. Sci. U.S.A.*, **106**, 18740–18744.
30. Fujita,S. *et al.* (2008) MiR-21 gene expression triggered by AP-1 is sustained through a double-negative feedback mechanism. *J. Mol. Biol.*, **378**, 492–504.
31. Qi,J. *et al.* (2012) MiR-365 regulates lung cancer and developmental gene thyroid transcription factor 1. *Cell Cycle*, **11**, 177–186.
32. Korkmaz,G. *et al.* (2012) MiR-376b controls starvation and mTOR inhibition-related autophagy by targeting ATG4C and BECN1. *Autophagy*, **8**, 165–176.
33. Shu,M. *et al.* (2011) MicroRNA 335 is required for differentiation of malignant glioma cells induced by activation of cAMP/protein kinase A pathway. *Mol. Pharmacol.*, **81**, 292–298.